



## Analysis of EEG signals and its application to neuromarketing

**Mahendra Yadava<sup>1</sup> · Pradeep Kumar<sup>1</sup> ·  
Rajkumar Saini<sup>1</sup> · Partha Pratim Roy<sup>1</sup> ·  
Debi Prosad Dogra<sup>2</sup>**

Received: 30 August 2016 / Revised: 8 February 2017 / Accepted: 6 March 2017 /

Published online: 18 March 2017

© Springer Science+Business Media New York 2017

**Abstract** Marketing and promotions of various consumer products through advertisement campaign is a well known practice to increase the sales and awareness amongst the consumers. This essentially leads to increase in profit to a manufacturing unit. Re-production of products usually depends on the various facts including consumption in the market, reviewer's comments, ratings, etc. However, knowing consumer preference for decision making and behavior prediction for effective utilization of a product using unconscious processes is called “Neuromarketing”. This field is emerging fast due to its inherent potential. Therefore, research work in this direction is highly demanded, yet not reached a satisfactory level. In this paper, we propose a predictive modeling framework to understand consumer choice towards E-commerce products in terms of “likes” and “dislikes” by analyzing EEG signals. The EEG signals of volunteers with varying age and gender were recorded while they browsed through various consumer products. The experiments were performed on the dataset comprised of various consumer products. The accuracy of choice prediction was recorded using a user-independent testing approach with the help of Hidden Markov

- 
- ✉ Pradeep Kumar  
pradeep.iitr7@gmail.com
  - Mahendra Yadava  
mahendray68@gmail.com
  - Rajkumar Saini  
rajkumarsaini.rs@gmail.com
  - Partha Pratim Roy  
proy.fcs@iitr.ac.in
  - Debi Prosad Dogra  
dpdogra@iitbbs.ac.in

<sup>1</sup> Department of Computer Science and Engineering, Indian Institute of Technology, Roorkee, India

<sup>2</sup> School of Electrical Sciences, Indian Institute of Technology, Bhubaneswar, India

Model (HMM) classifier. We have observed that the prediction results are promising and the framework can be used for better business model.

**Keywords** Neuroscience · Neuromarketing · Choice prediction · Consumer behavior · EEG

## 1 Introduction

Consumer commodity sector spends huge amount of money on advertising the usability or success of the products. This is necessary during pretesting of various alternative advertisement campaigns before launching and also during the in-market analysis of the campaign after launching.

A number of conventional methods exist to pretest advertisements. These methods include self-reported methods such as liking, recall or purchase intent, neuromarketing, etc. “Neuromarketing” phrase is the combination of two words “neuro” and “marketing”. This can be referred to as merging of two fields, namely “neuroscience” and “marketing”. Using neuroscience, it is possible to improve the marketing of the existing products. It provides an insight to improve the design of products before actual launch in the market [24]. Therefore, neuroscience reveals information about consumer preferences on products. This is not possible using traditional methods such as questionnaire, attitude or verbal communication. Thus, neuromarketing can help the product-companies to reduce expenditure on product advertisements.

Over the past few years, researchers have developed different neurophysiological methods for analyzing the consumer behavior and advertisement phenomenon to study different aspects of marketing [7, 20]. The growth has been recorded due to the technological advancement of instruments such as Functional magnetic resonance imaging (fMRI), Magnetoencephalography (MEG), and electroencephalography (EEG) often used in neuromarketing. fMRI is a neuroimaging technique used to measure the amount of deoxygenated hemoglobin during neuronal activity. It describes brain function with spatial and temporal resolutions of one millimeter and per second change, respectively [33]. The device has been used for grading user preferences on various applications.

Berns et al. [6] have used fMRI data to predict music popularity by measuring the brain activity of 27 adolescents. The authors have shown that the positive correlation of the participant's brain responses with the sales after three years. However, the cost associated with such experiments can be very expensive and often turns out to be in the order of several millions of dollars [35]. Moreover, additional costs such as insurance, maintenance and portability issues limit the use of fMRI in such applications. MEG is used to capture the brain activity that is caused by neuron activity. Such neuron activity creates a magnetic field that is amplified and mapped by MEG with spatio-temporal information. However, due to higher cost, technical complexities and limited access of subcortical regions for imaging, it is not preferred as a device to develop systems of neuromarketing.

To overcome some of the limitations of the above mentioned problems, we have used an inexpensive setup to examine the brain activity using EEG signals that offers a high temporal resolution and is cheaper than fMRI and incurs fewer electrodes (only 14), easy handling, wireless connectivity and lower maintenance cost. Such parameters extend the use of the device from laboratory to general practice. Generally, people do not want to fully express their feelings and preferences towards products when asked explicitly. However,

neuroimaging tools (i.e. EEG) and techniques are capable in accessing the customer brain's information during the generation of a preference or the observation towards a product. Therefore, such brain imaging techniques helps marketing researchers in decision making for further promotions of the products. Boksem and Smids [7] reported that the brain responses captured using EEG signals while users were watching movie trailers can provide valuable inputs for predicting population-level preferences of movies. In addition to the brain imaging, other physiological aspects such as eye tracking, heart rate or respiration [21, 30] can also be measured to relate with the consumer's experience. Motivated by the above research, we have developed an EEG enabled system that can easily replace costly setups of present day neuromarketing. Our main contributions are as follows:

1. Firstly, we present a Neuromarketing framework for predicting consumer preferences while they view E-commerce products by analyzing EEG signals.
2. Our second contribution is an experimental validation of the prediction using Hidden Markov Model (HMM) based sequential classifier. We also present a comparative analysis with other popular classifiers.

Rest of the paper is organized as follows. Section 2 provides an overview of the existing research. Next, we present preprocessing, feature extraction and classification methodology in Section 3. Results obtained using a custom-built dataset are presented in Section 4. In Section 5, we present the conclusion of the paper with possible future extensions.

## 2 Related work

In this section, we review the recent works that linked EEG signals activity in predicting the consumers behavior and emotions based on the self reported ratings. Initially, Ambler et al. [1] have exploited the relationship between the brain imaging and the consumer decision while watching a virtual video of supermarket visit. The subjects were asked to choose one of the three brands after 90 stops. The authors found improvement in predicting the product brand choice. The authors have recorded strong correlations between the brain activation in right parietal cortex with the subjects familiarity with the brand. In [19], the authors explored the brain activity of 18 subjects while making the internal decision of likes and dislikes for a set of products. Eye tracker was used to capture the user's choice from a set of three images displayed on the computer's screen and simultaneously the EEG signals were recorded. The authors have used Principal Component Analysis (PCA) and Fast Fourier Transformation (FFT) to analyze the changes in the main frequency bands. A significant change in the spectral activity with theta bands were recorded in the frontal, parietal and occipital areas while the participants were indicating their preference by computing mutual information between the users preference and different EEG bands. In [35], the authors predicted the choices of 10 consumer products using EEG signals recorded while the participants viewed the products on computer screen. In their second experiment, pair of the same products were shown to participants and EEG signals were recorded. They have found an increase in N200 component in the mid-frontal electrode and a correlation has also been reported between the theta band power and the preferred products.

Baldo et al. [5] have proposed a pre-market forecasting system for products using brain data. The authors have recorded EEG data of 40 participants while viewing the different shoes on the computer screen. The participants were asked either to buy the shoes or not after every presentation and also a questionnaire was given to fill with rating scale 1 to 5.

The authors have shown that classification of products using EEG signals were better than the rating based classification which were reported as 80% and 60%, respectively, when 30 pairs of shoes were classified into two classes. A recommendation system for E-commerce products was proposed in [10] by combining the pre-purchase and post-purchase ratings. The EEG signals were recorded while the participants viewing virtual 3D products. The pre-purchase ratings were computed automatically using the emotional states of participants using alpha and beta bands. The authors have used adapted collaborative filtering to implement the recommendation system.

Murugappan et al. [25] have proposed an FFT based neuromarketing system for predicting the most preferred automobile brand among four categories. The brain activity of 12 subjects have been recorded while watching the brand advertisement video. Butterworth band pass and Laplacian filter were used to preprocess the EEG signals and three statistical features i.e. power spectral density (PSD), spectral energy (SE) and spectral centroid (SC) have been extracted from alpha band spectrum. The subject intention for a brand was computed using k-Nearest-Neighbor (k-NN) and Probabilistic Neural Network (PNN) classifiers where an accuracy of 96.62% was recorded using PSD feature with PNN classifier. In [7], the authors proposed a consumer choice preference modeling framework for movie trailers using EEG signals. The authors have found that high frequencies i.e. beta and gamma were significant correlated to individual preferences and population preference. Soleymani et al. [30] have proposed an approach for affective ranking of movie scenes, which is based on both user's emotion and video content-based features. User emotions were inferred using five peripheral physiological signals and self-assessments. The authors found that the movie scenes were correlated with the user's self-assessed arousal and valence. Moreover, the study also suggests that peripheral physiological signals can also be used to characterize and rank video contents. In [18], the authors presented the effects of color preferences on the neural mechanisms by analyzing the changes in EEG oscillations while showing two colors on the computer screen for 1 second duration to 19 users. They have found an increment in the theta amplitudes when the preferred color was presented or selected by a user. In [20], the authors have shown different choice sets to 18 users to investigate the different brain activities during decision making using EEG signals and eye tracker device. The eye tracker was used to record the frequencies of choices. In order to discover the most relevant brain regions associated with the choice task, mutual dependence between the extracted sensor features and the corresponding class label of preference was performed. They have reported high synchronization between symmetric frontal and occipital brain regions with high values for theta, alpha and beta band waves.

In [34], the authors have proposed a learning assessment methodology using EEG signals by finding a correlation between the brain waves and the learnability of a software. They have considered that the software is learnable for subjects with dominant alpha waves. Holzinger et al. [14], have developed a stroke rehabilitation system using EEG signals. The electro-cortical activity was recorded from 120 channels and applied Independent Component Analysis (ICA) for separating multivariate signals into additive subcomponents. The authors have found patterns over the sensorimotor area that have been involved in the execution and association of movements. In [15], the authors have applied Approximate Entropy (ApEn) on electrocardiogram (ECG) data from 26 participants for evaluating the human concentration. In order to acquire useful information from ECG time series, the ApEn window was kept small for intra-subject information in comparison to inter-subject. For this, the authors have proposed the term *truthfulness* as a complement to the statistical validity of the ApEn windows and for the stability of ApEn distribution.

The Savitzky-Golay (S-Golay) filter is widely used for signal smoothing in various fields like elastography, EEG and magnetocardiogram. In [11], the authors have investigated the use of S-Golay filter in ECG signal processing. The best choice was found to use the quadratic smoothing and differentiation filter with 17 point length for 500 Hz sampling rate ECG signal processing. A two class motor imaginary-based BCI was proposed in [9] using EEG signals. The authors have proposed Recurrent Quantum Neural Network (RQNN) architecture to filter the EEG signals using quantum mechanics and Schrodinger wave equation. In [27], the authors have proposed a real time removal of eye blink artifacts from EEG signals using S-Golay filter. They have found the correct estimation of the blink signal with high correlation to the original blink signal. Next, an adaptive noise cancellation system was adopted to remove the blink effect from the EEG signals. A summary of the related work has been shown in Table 1.

### 3 System setup

In our framework, the system was setup as follows. Emotiv EPOC+ device has been used for capturing the EEG signals which is a neuro-signal data acquisition, wireless device.

**Table 1** Summary of the related work

Author & Year	Approach	No. of Channels	Dataset & Participants
Ambler et al. [1], 2004	MEG, Correlation features	–	3 products, 18 subjects
Khushaba et al. [19], 2012	EEG, eye-tracker, PCA and FFT	14	72 images, 18 subjects
Telpaz et al. [35], 2015	EEG, N200	–	10 products, n.a.
Baldo et al. [5], 2015	EEG, self-reports	64	30 pair of shoes, 40 subjects
Guo et al. [10], 2013	EEG, purchase ratings, alpha, beta bands and collaborative filtering	14	3D products, n.a.
Murugappan et al. [25], 2014	EEG, Butterworth, FFT, PSD, SE & SC using k-NN & PNN	14	4 Brands, 12 subjects
Boksem et al. [7], 2015	EEG, beta and gamma waves	64	56 movie trailers, 32 subjects
Kawasaki et al. [18], 2012	EEG, theta waves	60	2 colors, 19 subjects
Soleymani et al. [30], 2008	EEG, EMG, heartrate etc., self-assessed ratings, correlations	64	64 movie scenes, 8 subjects
Stickel et al. [34], 2007	EEG, alpha beta & gamma waves	3	32 subjects
Holzinger et al. [14], 2012	EEG, ICA, 3D electrode positions, MRI images	120	–
Holzinger et al. [15], 2012	ECG, ApEn, Butterworth filter	1	26 subjects
Proposed Methodology	EEG, DWT, S-Golay filter, HMM classifier	14	25 Male 15 Female subjects

A pictorial representation of EEG sensors layout over the scalp and the associated accessories is shown in Fig. 1. The device has 14 channels for EEG data that are located at AF3, F7, F3, FC5, T7, P7, O1, O2, P8, T8, FC6, F4, F8, AF4 positions as per the International 10 - 20 system as shown in Fig. 1a [20]. The electrodes that are located above the ears i.e. CMS and DRL are called reference electrodes. Internally an EPOC is sampled at a frequency of 2048 Hz that is down-sampled to 128 Hz sampling frequency per channel. The data is sent to a computer using Bluetooth connectivity by utilizing a USB dongle. Before use, felt-pads that lie on top of sensors must be moistened using a saline solution. The device battery is recharged using a USB charger. The sensor along with the USB bluetooth dongle, sensor felt-pads, saline solution and charger cable are shown in Fig. 1b.

EEG sensor was mounted onto the head of participants and asked to view shopping items as shown in Fig. 2, where a user was viewing an item in computer screen. A flow diagram of the proposed approach can be seen in Fig. 3. At first during enrollment phase, EEG signals were captured simultaneously when the user was viewing an item. After viewing, the user was asked for his preference of the product in terms of two classes i.e. like or dislike. Then, the signal goes through certain signal preprocessing and feature extraction steps. For feature extraction Discrete Wavelet Transform (DWT) based features have been extracted. Next, classification models are built according to the ground truth made by user's choice. In the testing phase, a recorded test sample is preprocessed and decomposed into frequency bands for feature extraction and tested against the trained model. The results were carried out in two classes namely, like and dislike, corresponding to a particular viewing item. The detailed description of preprocessing, wavelet decomposition and feature extraction are discussed in Section 3.1.

### 3.1 Preprocessing and feature extraction

In this section, we present the details of the signal smoothing technique that is used to preprocess the signal for feature extraction. Next, Discrete Wavelet Transform (DWT) based wavelet analysis has been performed to extract valuable features from the recorded signals.

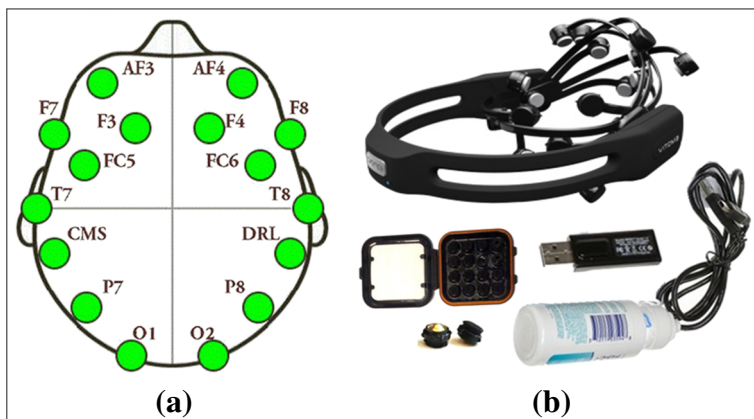


**Fig. 1** EEG brain sensor details (a) Sensor layout on the skull (b) Emotiv EPOC+ sensor along with the associated accessories



**Fig. 2** System setup where a user watching consumer products during experiment

### 3.1.1 Savitzky-Golay (S-Golay) filter

S-Golay filter has been used successfully by researchers in signal smoothing [4, 11, 17, 27]. It is a least square or polynomial based filter that smooths the noisy signal by fitting consecutive subsets of neighboring signal points using low degree polynomial and linear least squares. From a signal  $S_j = f(t_j)$ , ( $j = 1, 2, \dots, n$ ) having length  $n$ , S-Golay filter can be computed using (1).

$$Q_j = \sum_{i=-\frac{m-1}{2}}^{\frac{m-1}{2}} c_i S_{j+i}, \quad \frac{m+1}{2} \leq j \leq n - \frac{m-1}{2} \quad (1)$$

where,  $m$  represents the frame span,  $c_i$  denotes the number of convolution coefficients and  $Q$  is smoothed signal. The frame span  $m$  is used to compute the values of  $c_i$  with a polynomial. In this work, the filter has been applied to smooth EEG signals using a frame span of size 5 with a quadratic polynomial. The computed values for  $c_i$  are -3, 12, 17, 12, and -3.

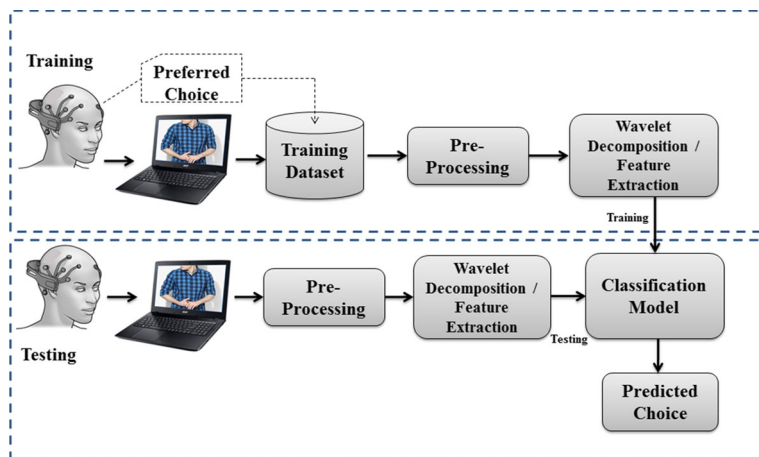


**Fig. 3** Flow diagram of the proposed EEG based consumer's choice prediction model

The signal smoothing process is shown in Fig. 4, where Fig. 4a shows a raw EEG signal of a participant and Fig. 4b shows the corresponding smooth signal after applying the filter.

### 3.1.2 Discrete wavelet transform (DWT) based features

DWT is widely used in biomedical signal processing [2] because it represents a signal in time-frequency domain. The basic idea in DWT is to convert an input signal into a series of small waves using multistage decomposition. The wavelet transformation based analysis of a signal can be performed at different frequency bands by decomposing it into approximation ( $A$ ) and detail ( $D$ ) coefficients. A schematic decomposition of an EEG signal is shown in Fig. 5, where the signal first passes through two digital filters i.e. Low pass filter ( $L$ ) and High pass filter ( $H$ ). Low-pass filter ( $L$ ) removes high-frequency fluctuations from the signal and preserves slow trends. The outputs of low-pass filters provide an approximation ( $A$ ) of the signal. High-pass filter ( $H$ ) removes the slow trends from the signal and preserves high-frequency fluctuations. The output of the high-pass filter provides the detail ( $D$ ) information about the signal that is also called wavelet coefficients. In order to get the detail coefficients at next level the approximation coefficients must be passed again to  $L$  and  $H$  filters as shown in Fig. 5 and so on. A wavelet function is defined using (2 and 3).

$$\int_{-\infty}^{+\infty} \psi(t) dt = 0 \quad (2)$$

$$\psi_{m,n}(t) = a_0^{-m/2} \psi(a_0^{-m}t - nb_0) \quad (3)$$

where  $a$  and  $b$  are the scaling and translation parameters, respectively. These parameters are having discrete values. The variables  $m$  and  $n$  are the frequency and time location that belong to  $Z$ . By choosing  $a_0 = 2$  and  $b_0 = 1$  provide a basis of multi-resolution analysis which decomposes a signal into approximation and details coefficients [2]. The computation

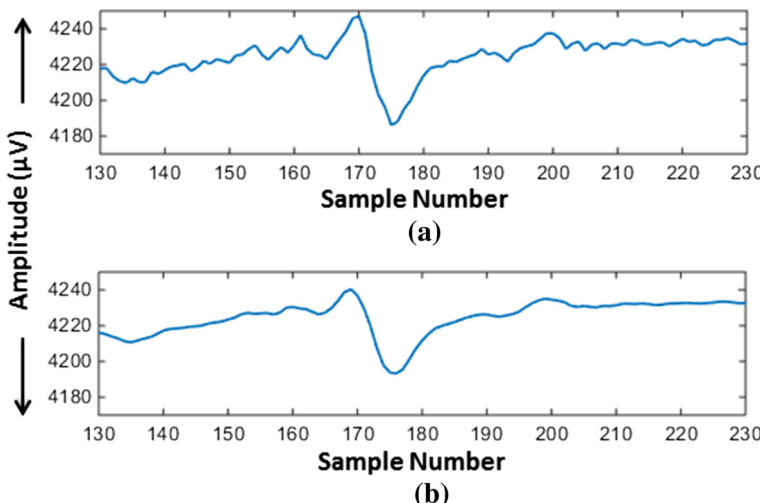


**Fig. 4** Example of signal preprocessing. **a** Raw EEG signal **(b)** Smoothed signal

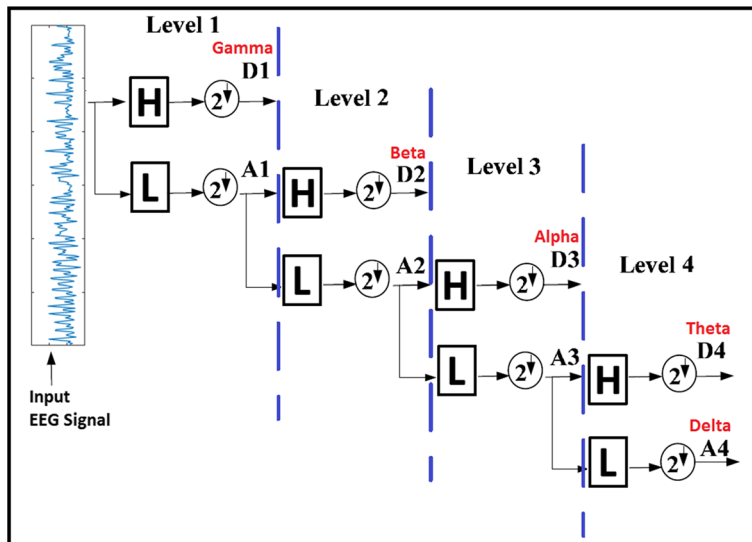


**Fig. 5** Different levels of Wavelet decomposition using DB4 plotted for a single channel ‘AF4’

of the approximation and detail coefficients are performed by using scaling and wavelet function as represented in (4) and (5), respectively.

$$\phi_{j,k}(n) = 2^{j/2} h(2^j n - k) \quad (4)$$

$$\omega_{j,k}(n) = 2^{j/2} g(2^j n - k) \quad (5)$$

where  $\phi_{j,k}(n)$  and  $\omega_{j,k}(n)$  are the scaling and wavelet functions that belongs to  $L$  and  $H$ , respectively. The variable  $n \in [0, 1, 2, \dots, M - 1]$ ,  $M$  is the length of the signal,  $k$  and  $j$  takes the value from 0 to  $J - 1$ , where  $J = \log_2(M)$ . The values of  $A_i$  and  $D_i$  are obtained when the signal passed through  $L$  and  $H$ , respectively. Similarly, the values of  $A_i$  and  $D_i$  at the  $i^{th}$  level are computed using (6) and (7), respectively.

$$A_i = \frac{1}{\sqrt{M}} \sum_n x(n) \times \phi_{j,k}(n) \quad (6)$$

$$D_i = \frac{1}{\sqrt{M}} \sum_n x(n) \times \omega_{j,k}(n) \quad (7)$$

In this work, we have used four level of EEG signal decomposition by using the Daubechies 4 (DB4) wavelet decomposition technique as shown in Fig. 5. The DB4 decomposition results into a group of five wavelet coefficients, where each group corresponds to a frequency band that represents brain electrical activity i.e.  $D_1$ ,  $D_2$ ,  $D_3$ ,  $D_4$  and  $A_4$ . These groups correlate with the EEG spectrum having four different frequency bands which consist of delta (1–4 Hz), theta (4–8 Hz), alpha (8–13 Hz), beta (13–22 Hz) and Gamma (32–100 Hz). A number of work have exploited the theta band power during a preference judgment tasks [18–20]. Vecchiato et al. [36] analyzed the cortical activity in the left hemisphere using theta band during the observation of TV commercials. A graphical representation of the five band waves is shown in Fig. 6b–f correspond to a smoothed EEG signal shown in Fig. 6a.

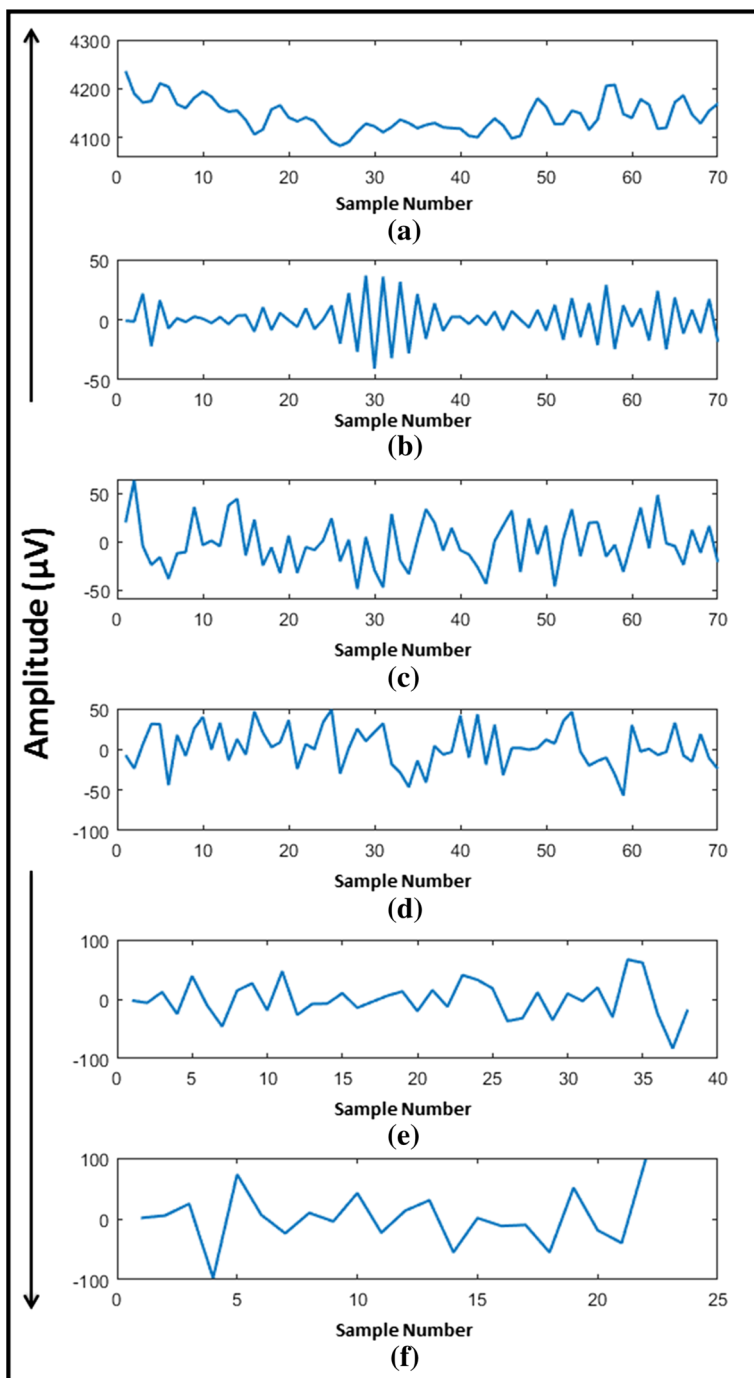


**Fig. 6** Feature extraction in the form of different waves for a smoothed signal. **a** Smoothed signal **(b)** Gamma band oscillations **(c)** Beta band oscillations **(d)** Alpha band oscillations **(e)** Theta band oscillations **(f)** Delta band oscillations

The computation has been done for all 14 channels of the EEG signals that result into a 14 dimensional feature vector corresponding to each band i.e. gamma, beta, alpha, theta and delta which are denoted by  $F_g$ ,  $F_b$ ,  $F_a$ ,  $F_t$  and  $F_d$ , respectively.

### 3.2 HMM based consumer choice classification

Hidden Markov Model (HMM) is widely used to model the time-series data [22]. The model is successfully used by researchers in building Brain-Computer-Interface (BCI) applications using EEG signals including mental task classification [31], eye movement tracking [16] and medical applications [37]. HMM is described as  $\lambda = (\pi_c, A_c, B_c)$  [26], where

- $\pi_c$  is the initial distribution for class  $c$ .  $c = 1, 2, \dots, C$ ,  $\sum_{c=1}^C \pi_c = 1$ ,
- $A_c$  is a  $S \times S$  state transition probability, and
- $B_c$  is the output probability matrix for the class  $c$ . The matrix contains the probability information from a state and observing a symbol belongs to observation sequence  $Ob$ .
- For each  $\lambda_c$ , the posterior  $P(\lambda_c|Ob)$  can be estimated for observation  $Ob$  likely to be assigned to one of the class  $C$ .
- The most probable class  $C^*$  can be estimated as given in (8) [23].

$$C^* = \arg \max_c P(\lambda_c|Ob) \quad (8)$$

such that,

$$P(\lambda_c|Ob) = \frac{P(Ob|\lambda_c)P(\lambda_c)}{P(Ob)} \quad (9)$$

where,  $P(Ob)$  is the evidence that is calculated using (10).

$$P(Ob) = \sum_1^C P(Ob|\lambda_c)P(\lambda_c) \quad (10)$$

The HMM models are trained separately for each feature vector i.e. using  $F_g$ ,  $F_b$ ,  $F_a$ ,  $F_t$  and  $F_d$ . Re-estimation of the initial output probabilities is done using Baum-Welch algorithm whereas the prediction of the users choice is performed using Viterbi decoding algorithm by finding the best likelihood for a given sequence.

## 4 Results

In this section, we present the results of the choice prediction that have been computed over the dataset collected to test the proposed framework. The results were computed in a user-independent based training approach by HMM. By user-independent, it means that predicting a user's choice does not require his/her training data. The prediction results were carried out using leave-one-out cross validation approach. Next, a comparative analysis is performed with SVM classifier and other state of the art techniques.

### 4.1 Dataset description

The EEG signals using all 14 channels have been recorded from 25 participants while viewing consumer products on computer screen. All the participants are of age between 18 to

38 years who belong to Indian Institute of Technology, Roorkee, India. A collection of 14 different products have been chosen where each product has three different varieties which create 42 ( $14 \times 3$ ) different product images. Thus, a total of 1050 (i.e.  $42 \times 25$ ) EEG signals have been recorded for all participants. The feedback response in form of like/dislike was collected from the subjects for each image in the collection. Each image was displayed for 4 seconds and EEG signals were recorded in parallel. After showing each image the choice preference of the user was recorded. During our data collection, we have instructed the users to provide their correct choices towards products. A description of the dataset along with the product name and image with their varieties are shown in Table 2. The dataset is made public<sup>1</sup> for the prospective research community.

Figure 7 shows the variation in the EEG signals of three different participants for the same product as per their choices for the product. Figure 7a and b indicate the details of the products when viewed by same set of users. The first column of the figure shows the brain activity signal, column 2 shows the product image, column 3 shows the brain activity map plotted for theta band and column 4 shows the choice preference of the the participants after viewing the product. The brain activity map shows the activity in the frontal part of the brain as represented by the heat-map in figure. Similarly, the variation in the EEG signals of the same user for different products is depicted in Fig. 8.

## 4.2 Consumer choice classification

Here, we present the choice preference results using the sequential HMM classifier. The model is built by learning from the EEG samples of ( $N - 1$ ) subjects and then testing the trained model using  $N^{th}$  subject brain samples. The said policy has been applied for all the subjects in the experiments. Finally, the average performance is reported in terms of accuracy. The performance of the framework has been carried out by varying number of HMM states i.e.  $S_t \in \{3, 4, 5, 6, 7\}$  and varying the number of Gaussian mixture components per state i.e. 1 to 128 with an incremental step of power of 2. The model has been trained separately for bands  $F_g$ ,  $F_b$ ,  $F_a$ ,  $F_t$  and  $F_d$ . The results are shown in Figs. 9 and 10 by varying GMM components and HMM states, respectively. A highest prediction rate of 70.33% has been recorded at 8 Gaussian mixtures components and 3 HMM states with theta band features ( $F_t$ ) in comparison to other feature bands based prediction results. In this work, due to the two class problem of users choice, best accuracies are recorded with lower number of GMMs and HMMs states.

In addition to this, the prediction results are also computed for each product types as shown in Fig. 11. It can be observed from the figure that the highest prediction is achieved as 95.33% for the product category ‘Shoe’ whereas lower prediction rate of 52% has been recorded for the products ‘School Bag’, ‘Belt’, ‘Sun Glass’ and ‘Sweater’. The prediction of choice preferences has also been computed individually for all 25 participants. See Fig. 12, where the maximum and minimum prediction rate of 83.09% and 60.08% are recorded for users ‘s3’ and ‘s2’, respectively.

Experiments are also conducted to find the dominating EEG channels corresponding to different brain lobes for consumer choice prediction. The performance has been measured according to 4 different brain lobes namely, Frontal (AF3,AF4,F3,F4,F7,F8), Parietal (P7,P8), Occipital (O1,O2) and Temporal (T7,T8). The accuracies of the different brain lobes are shown in Fig. 13. The maximum accuracy has been recorded by considering all

<sup>1</sup><https://sites.google.com/site/iitrcsepradeep7/>



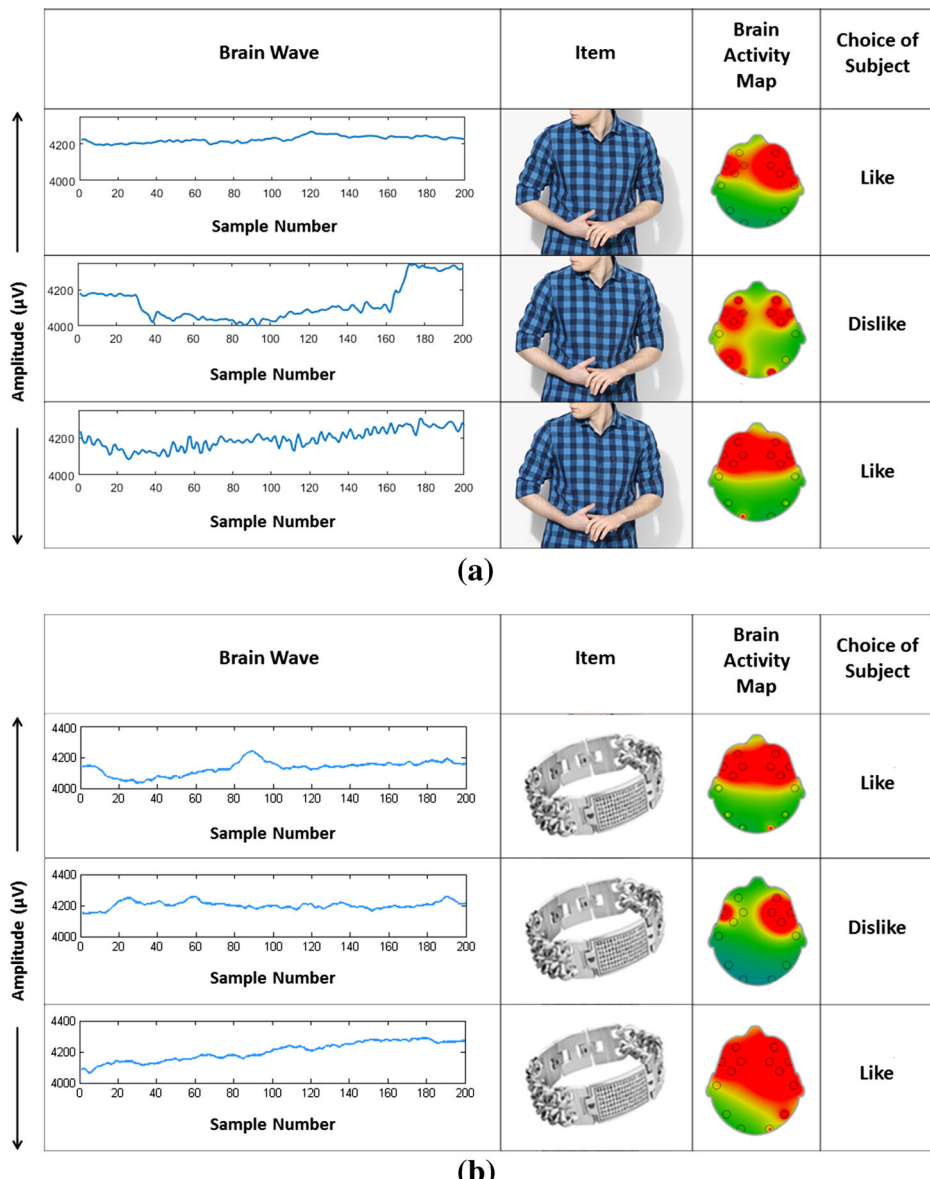


**Fig. 7** EEG signal examples of three different users when they viewed the same product. **a** and **(b)** indicate details of two different products when viewed by same set of users. Column-wise details are as follows. (i) EEG signal response against channel ‘AF4’ (ii) Product viewed by three different users (iii) Brain activity map while watching the products (iv) The choice preference for the product

hyperplane separates the classes. The training data  $\{x_i, y_i\}$  for  $i = 1, \dots, m$  and  $y_i \in (-1, 1)$  must satisfy (11) and (12),

$$wx_i + b \geq +1 \text{ for } y_i = +1 \quad (11)$$

$$wx_i + b \leq -1 \text{ for } y_i = -1 \quad (12)$$

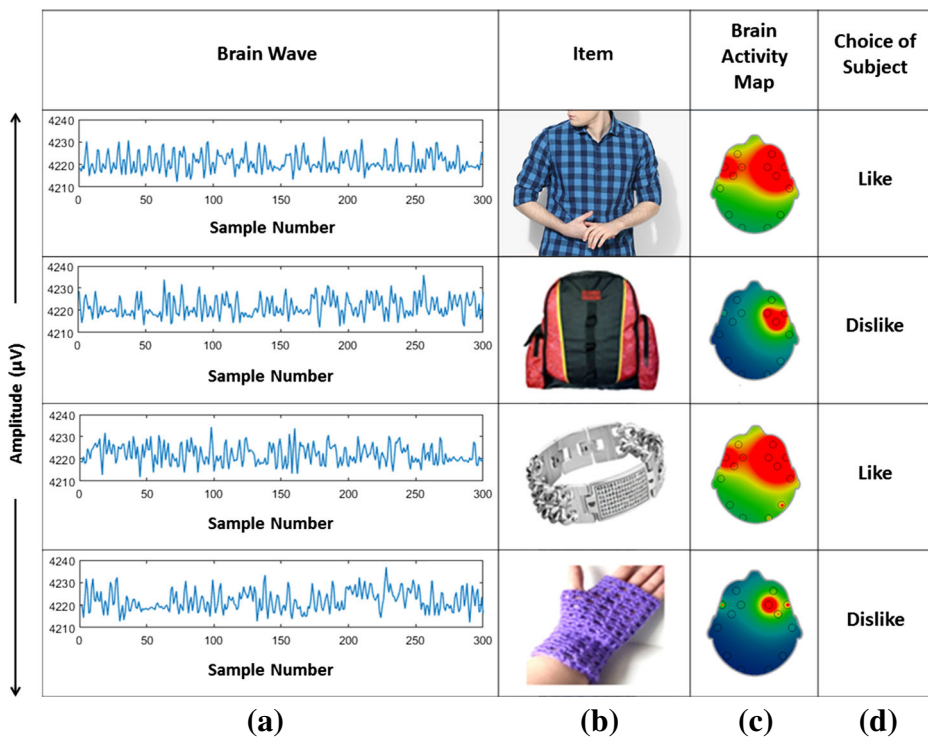


**Fig. 8** EEG signal examples for the same user (column-wise): (a) EEG signal responses against channel ‘AF4’ (b) Product type (c) Brain activity map (d) Preferred choice

where  $w$  is the hyperplane parameter and  $b$  denotes the offset. SVM finds a decision boundary that maximizes the distance between two hyperplanes termed as margin. Thus, finding

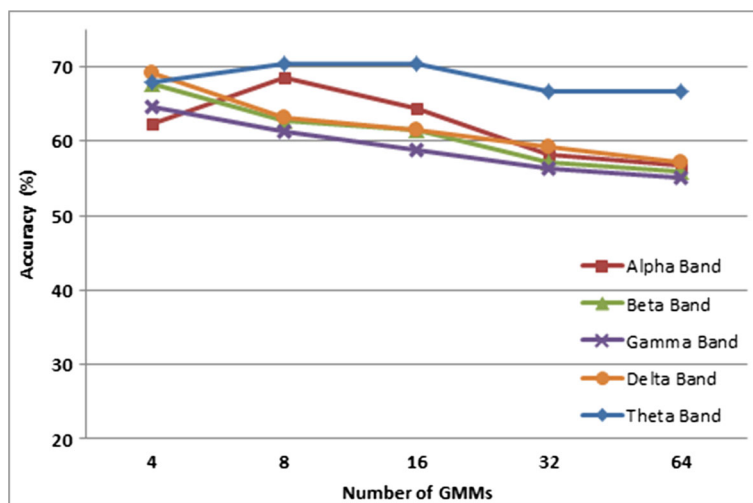


**Fig. 9** HMM based user choice classification by varying number of Gaussian mixtures

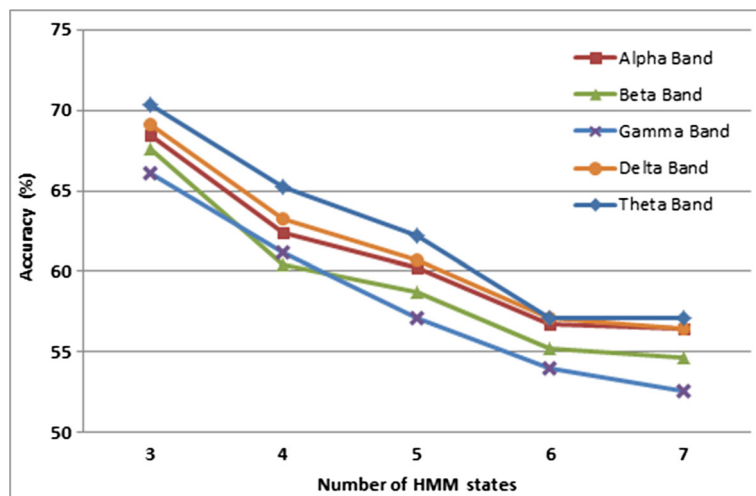


**Fig. 10** User choice classification by varying number of HMM states

the decision boundary is an optimization problem to minimize  $\|w\|^2$  which is solved by using Lagrange optimization framework. The general solution is represented by (13). In case of non-linear classification, the general solution is represented by (14), where  $k$  is the kernel function on behalf of which SVM provides both linear and non-linear classification functionality.

$$f(x) = \sum_i a_i y_i (x_i, x) \quad (13)$$

$$f(x) = \sum_i a_i y_i k(x_i, x) \quad (14)$$

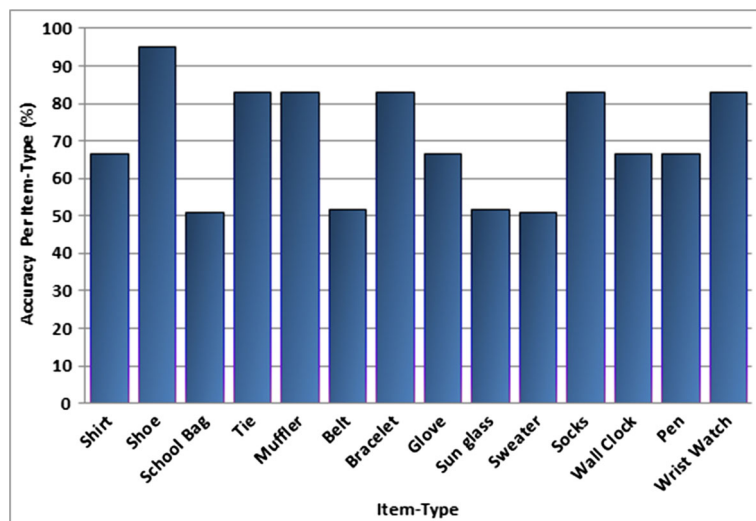


**Fig. 11** An average prediction performance for each product from the dataset

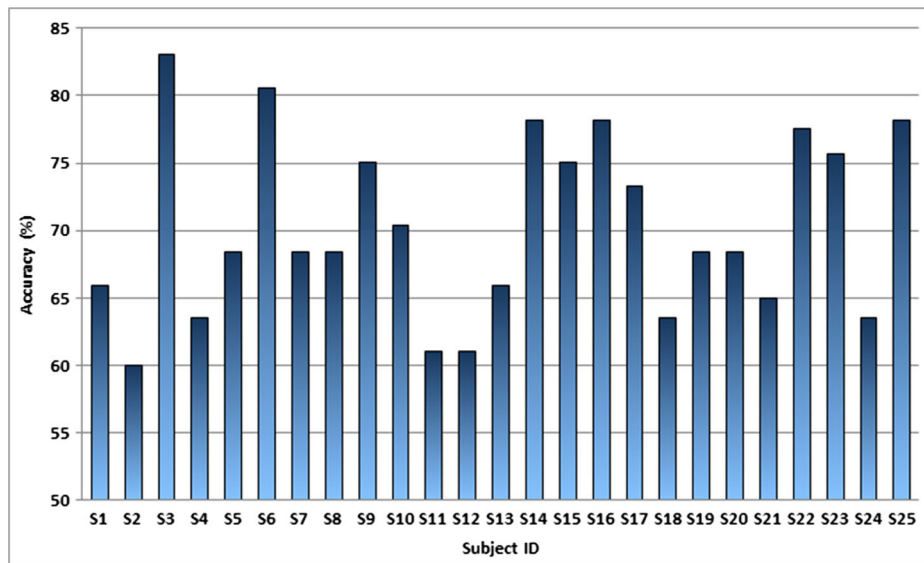


**Fig. 12** User-wise prediction of preferences for all products in the dataset

RF consists a number of trees that are grown randomly. The leaf node of each tree estimated with the posterior distribution over the like/dislike. The internal nodes of the tree contain a test that is used to split the space for the testing data. The binary test at each node is chosen either randomly or by using greedy algorithm that picks the test set to separate using information gain defined in (15)

$$\Delta E = - \sum_i \frac{|R_i|}{|R|} E(R_i) \quad (15)$$

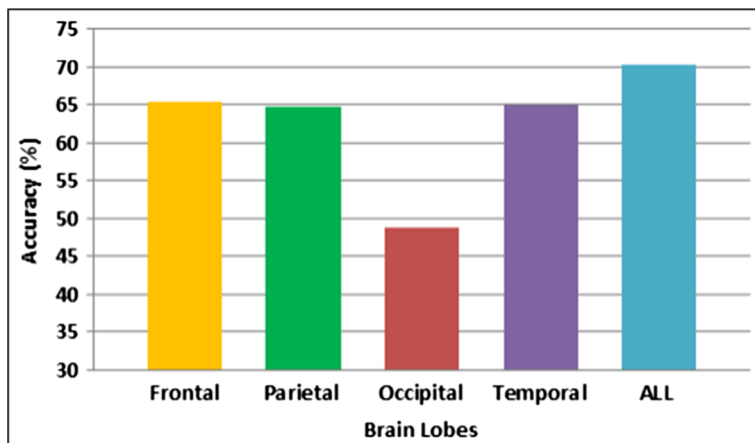


**Fig. 13** User-wise prediction of preferences for different brain lobes

where  $R$  is the training set of examples partitioned into two subsets  $R_i$  as per the test and  $E(R)$  is the entropy computed using (16), where  $P_j$  denotes the proportions of  $R$  belongs to class  $j$ . The process repeated for each internal node and stops after reaching a given depth.

$$E(R) = - \sum_{j=1}^N P_j \log_2(P_j) \quad (16)$$

If,  $T$ ,  $C$  and  $L$  represent the set of trees, classes and the leaves, then estimation of the posterior probabilities ( $P_{t,l}(Y(E) = c)$ ) where  $c \in C$ ,  $t \in T$  and  $l \in L$ .  $Y(E)$  represents the class label  $c$  for the training sample  $E$ . For testing, the test sample passed down until it reaches to the leaf node where all the posterior probabilities are averaged and the classification is done using argmax rule.

ANN classifier has been considered to be good for the classification of EEG signals by various researchers [3, 32]. The classifier has been associated with inherent properties like adaptive learning, robustness, self-organization, and generalization capability. In this work, we have implemented a feed-forward neural network with two hidden layers and one output layer. The network has been trained with error backpropagation algorithm. Sigmoid function has been considered as activation function for all units. Random small values have been used to initialized all weights followed by gradient-descent search in the network's weight space for a minimum of a squared error function of the network's output. The error is defined as the network's output and the target value for each input vector.

Four statistical features, namely, Mean (M), Standard Deviation (SD), Energy (EN) and Root-Mean-Square (RMS) have been extracted using the feature vector ( $F_t$ ) discussed in Section 3.1.2. The features have been computed using (17)–(20).

$$M = \frac{1}{n} \sum_{i=1}^n x_i \quad (17)$$

where  $x_i$  is the  $i^{th}$  sample of the data sequence and  $n$  denotes total number of data points.

$$SD = \sqrt{\frac{1}{n-1} \sum_{i=1}^n (x_i - \bar{x})^2} \quad (18)$$

where  $\bar{x}$  is the mean of the sample and  $n$  denotes the number of items in the sample.

$$EN = D \sum_{i=0}^{n-1} x_i^2 \quad (19)$$

where  $D$  is duration of signal, and  $x_i$  is discrete samples of the signal at regular intervals (0 to n-1).

$$RMS = \sqrt{\frac{\sum_{i=1}^n x_i^2}{n}} \quad (20)$$

where  $x_i$  is the  $i^{th}$  item of the sequence and  $n$  is the number of items in the sequence. A new feature vector of 56 dimensions have been formed corresponding to all 14 channels. For SVM, Linear kernel has been employed to evaluate the performance by varying the regularization parameter ( $C$ ). An accuracy of 62.85% has been recorded with SVM classifier with

C=6. The RF classifier requires the estimation of two parameters for developing a prediction model i.e. number of classification ( $m$ ) and the number of prediction variables ( $k$ ) [28]. The experiment has been carried out by varying  $m$  from 1 to 100 and by keeping the value of  $k$  as constant to 7. An average accuracy of 68.41% has been recorded at  $m=3$ . For ANN, the feed-forward network has been trained with two hidden layers and Sigmoid activation function. A comparison has been shown along with the standard deviation, average, maximum and minimum accuracies in Fig. 14, where the HMM based choice prediction model performs better than the other three. The performance has also been measured by slicing EEG signals into different time durations as shown in Fig. 15, where maximum accuracy has been recorded using the EEG signals of 4 seconds with HMM classifier.

#### 4.5 Impact of age and gender on choice prediction

In order to show the effectiveness of the proposed framework on different genders and age groups, we have additionally collected the EEG signals of 15 female candidates along with 25 male while watching the products. Results have been computed on theta band features ( $F_7$ ) with the help of HMM classifier. Gender-wise choice prediction performance is depicted in Fig. 16, where results of male candidates are better than female candidates by a margin of 4.77%. It could be due to dense hair of female subjects that cause additional noise in the incoming signals. The process also takes time to adjust the headset on female scalp.

Similarly, age-wise results have also been computed by dividing the dataset into three age categories. The details of the age categories is presented in Table 3. Choice prediction accuracies of all three categories are shown in Fig. 17, where highest results were recorded in age group ‘C’.

#### 4.6 Scalability test

Scalability test has been performed to analyze the impact of number of users on the proposed consumer choice prediction framework. For this, we have tested the system performance by varying number of users (including both male and female) in training i.e. from 5 to 40 users. The prediction performance is depicted in Fig. 18, where the system performance becomes almost stable after 35 users.

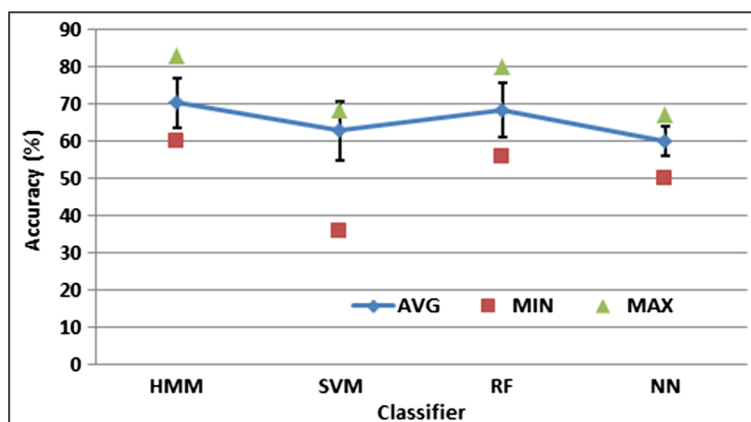


**Fig. 14** Comparative performance analysis among four classifiers for consumer choice prediction modeling

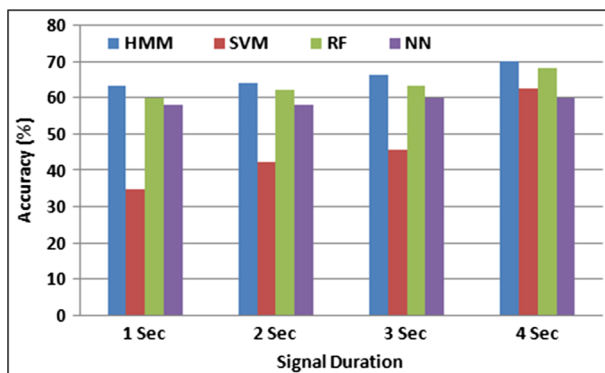


**Fig. 15** User choice classification by varying EEG signal duration

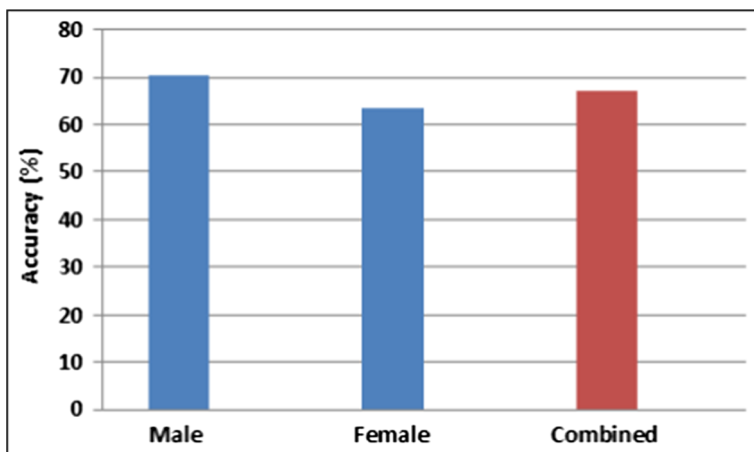


**Fig. 16** Gender-wise user choice classification

**Table 3** Description of aging groups for the analysis of choice prediction

Age-Group	Year	Male	Female	Total
A	18-23	10	6	16
B	25-30	8	5	13
C	>31	7	4	11

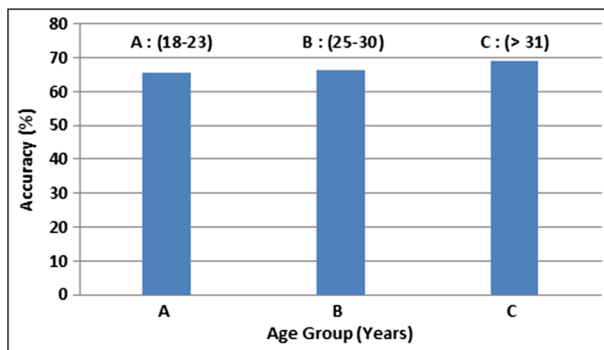


**Fig. 17** User choice classification in different age-groups

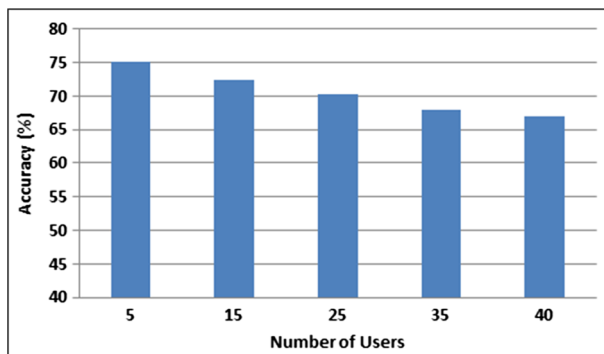


**Fig. 18** User choice prediction performance by varying number of users in training

**Table 4** Comparative analysis with existing consumer choice prediction work

Author & Year	Approach	Imaginary Tool & Dataset	Number of Subjects	Accuracy (%)
Smith et al. [29], 2014	Smoothing by Gaussiakernel, BayesianRegression	fMRI and 50 pairs of snacks	35	68.2%
Telpaz et al. [35] 2015	cardinal analysis	EEG and 10 products	—	65%
Proposed Methodology	Smoothing by S-Golay, HMM classifier	EEG and 42 product images	25 Male 15 Female	70.33% 63.56%

#### 4.7 Comparison with existing techniques

We have compared our system by some existing user preference based state of the art research works as shown in Table 4. It can be seen from the table that the proposed method outperforms existing ones.

### 5 Conclusion

In this paper, we have applied neuroscience to predict the choice preference of a user for a product using EEG signals. The brain activity of 40 participants comprised of 25 male and 15 female have been recorded while viewing products. Next, the signals have been smoothed and classified using HMM classifier. The result shows the effectiveness of the proposed framework and provides a complementary solution to the traditional measures of predicting the product success in the market. The framework could be used in developing market strategies, research and predicting market success by extending the existing models. In our study we did not analyze fake answer towards product preference. Thus, approaches to deal with fake responses could be studied in future work. Moreover, a neutral choice for the products could also be employed to provide more preferences to the users. The tracking of user's eye movement while watching products could be viewed as another parameter in predicting preferred choices. More robust features and classifier combination could be explored to improve the prediction results.

**Acknowledgments** The authors would like to thank the anonymous reviewers for their constructive comments and suggestions to improve the quality of the paper.

### References

1. Ambler T, Braeutigam S, Stins J, Rose S, Swithenby S (2004) Salience and choice: neural correlates of shopping decisions. *Psychol Market* 21(4):247–261
2. Amin HU, Malik AS, Ahmad RF, Badruddin N, Kamel N, Hussain M, Choi WT (2015) Feature extraction and classification for EEG signals using wavelet transform and machine learning techniques. *Aust Phys Eng Sci Med* 38(1):139–149
3. Anderson CW, Sijercic Z (1996) Classification of EEG signals from four subjects during five mental tasks. In: Solving engineering problems with neural networks: proceedings of the conference on engineering applications in neural networks (EANN'96), pp 407–414
4. Awal MA, Mostafa SS, Ahmad M (2011) Performance analysis of savitzky-golay smoothing filter using ECG signal. *Int J Comput Inf Technol* 1(02)
5. Baldo D, Parikh H, Piu Y, Müller KM (2015) Brain waves predict success of new fashion products: A practical application for the footwear retailing industry. *J Creat Value* 1(1):61–71
6. Berns G, Moore SE (2010) A neural predictor of cultural popularity. Available at SSRN 1742971
7. Boksem MA, Smidts A (2015) Brain responses to movie trailers predict individual preferences for movies and their population-wide commercial success. *J Mark Res* 52(4):482–492
8. Cortes C, Vapnik V (1995) Support-vector networks. *Mach Learn* 20(3):273–297
9. Gandhi V, Prasad G, Coyle D, Behera L, McGinnity TM (2014) Quantum neural network-based EEG filtering for a brain–computer interface. *IEEE Trans Neural Networks Learn Syst* 25(2):278–288
10. Guo G, Elgendi M (2013) A new recommender system for 3d e-commerce: an EEG based approach. *J Adv Manag Sci* 1(1):61–65
11. Hargittai S (2005) Savitzky-golay least-squares polynomial filters in ECG signal processing. In: Computers in cardiology, pp 763–766
12. Hazarika N, Chen JZ, Tsui AC, Sergejew A (1997) Classification of EEG signals using the wavelet transform. In: 13th International conference on digital signal processing proceedings, vol 1, pp 89–92





**Mahendra Yadava** is pursuing his M.Tech in Department of Computer Science at IIT Roorkee, India. His research interest includes Predictive Analysis and Signal Processing.



**Pradeep Kumar** is pursuing Ph D in Department of Computer Science at IIT Roorkee, India. His research interest includes Gesture Recognition and Machine Learning.



**Rajkumar Saini** is pursuing his PhD in Department of Computer Science at IIT Roorkee, India. His research interest includes Pattern Recognition, Machine Learning.



**Partha Pratim Roy** received his Ph.D. degree in computer science in 2010 from Universitat Autònoma de Barcelona, (Spain). He worked as postdoctoral research fellow in the Computer Science Laboratory (LI, RFAI group), France and in Syncromedia Lab, Canada. Presently, Dr. Roy is working as Assistant Professor at Indian Institute of Technology (IIT), Roorkee. His main research area is Pattern Recognition.



**Debi Prosad Dogra** is presently working as Assistant Professor in the School of Electrical Sciences of IIT Bhubaneswar. Earlier, he worked with various R&D organizations in India and abroad. He has obtained his doctorate degree in Computer Science & Engineering from IIT Kharagpur. His research interest includes video object tracking, visual surveillance, gesture recognition, augmented reality, and computer vision guided healthcare automation.

## Terms and Conditions

Springer Nature journal content, brought to you courtesy of Springer Nature Customer Service Center GmbH (“Springer Nature”).

Springer Nature supports a reasonable amount of sharing of research papers by authors, subscribers and authorised users (“Users”), for small-scale personal, non-commercial use provided that all copyright, trade and service marks and other proprietary notices are maintained. By accessing, sharing, receiving or otherwise using the Springer Nature journal content you agree to these terms of use (“Terms”). For these purposes, Springer Nature considers academic use (by researchers and students) to be non-commercial.

These Terms are supplementary and will apply in addition to any applicable website terms and conditions, a relevant site licence or a personal subscription. These Terms will prevail over any conflict or ambiguity with regards to the relevant terms, a site licence or a personal subscription (to the extent of the conflict or ambiguity only). For Creative Commons-licensed articles, the terms of the Creative Commons license used will apply.

We collect and use personal data to provide access to the Springer Nature journal content. We may also use these personal data internally within ResearchGate and Springer Nature and as agreed share it, in an anonymised way, for purposes of tracking, analysis and reporting. We will not otherwise disclose your personal data outside the ResearchGate or the Springer Nature group of companies unless we have your permission as detailed in the Privacy Policy.

While Users may use the Springer Nature journal content for small scale, personal non-commercial use, it is important to note that Users may not:

1. use such content for the purpose of providing other users with access on a regular or large scale basis or as a means to circumvent access control;
2. use such content where to do so would be considered a criminal or statutory offence in any jurisdiction, or gives rise to civil liability, or is otherwise unlawful;
3. falsely or misleadingly imply or suggest endorsement, approval , sponsorship, or association unless explicitly agreed to by Springer Nature in writing;
4. use bots or other automated methods to access the content or redirect messages
5. override any security feature or exclusionary protocol; or
6. share the content in order to create substitute for Springer Nature products or services or a systematic database of Springer Nature journal content.

In line with the restriction against commercial use, Springer Nature does not permit the creation of a product or service that creates revenue, royalties, rent or income from our content or its inclusion as part of a paid for service or for other commercial gain. Springer Nature journal content cannot be used for inter-library loans and librarians may not upload Springer Nature journal content on a large scale into their, or any other, institutional repository.

These terms of use are reviewed regularly and may be amended at any time. Springer Nature is not obligated to publish any information or content on this website and may remove it or features or functionality at our sole discretion, at any time with or without notice. Springer Nature may revoke this licence to you at any time and remove access to any copies of the Springer Nature journal content which have been saved.

To the fullest extent permitted by law, Springer Nature makes no warranties, representations or guarantees to Users, either express or implied with respect to the Springer nature journal content and all parties disclaim and waive any implied warranties or warranties imposed by law, including merchantability or fitness for any particular purpose.

Please note that these rights do not automatically extend to content, data or other material published by Springer Nature that may be licensed from third parties.

If you would like to use or distribute our Springer Nature journal content to a wider audience or on a regular basis or in any other manner not expressly permitted by these Terms, please contact Springer Nature at

[onlineservice@springernature.com](mailto:onlineservice@springernature.com)